Reac Kinet Mech Cat (2015) 114:529–545
DOI 10.1007/s11144-014-0798-8

An alternative approach for the screening of catalytic empty fruit bunch (EFB) pyrolysis using the values of activation energy from a thermogravimetric study

Alina Rahayu Mohamed · Zainab Hamzah

Received: 8 July 2014 / Accepted: 16 October 2014 / Published online: 30 October 2014

Abstract The catalytic effect of a series of doped and undoped metal oxides on the pyrolysis kinetics of empty fruit bunch (EFB) is investigated using thermogravimetric analysis (TGA) under nitrogen atmosphere and dynamic non-isothermal conditions from 301 to 1,273 K programmed at 10 K min^{-1}. The kinetic parameters, namely the activation energy (E_a) values and pre-exponential factor (Ln A) are determined based on the Coats–Redfern method. Segmentation of the TG data into two temperature regimes, which are 473–573 K (section I) and 573–613 K (section II) representing the hemicellulose and cellulose decomposition respectively. The effect of each catalyst on EFB pyrolysis is evaluated based on the calculated mean E_a for section I and section II which indicates that Al_2O_3 catalyzed EFB reaction reduces the E_a for section I and section II by 6.05 and 1.77 kJ mol^{-1}, respectively. Based on the E_a value for section I, Al_2O_3 is selected as the catalyst for incorporation in catalytic EFB pyrolytic reaction performs in a fixed bed reactor at 773 K with a heating rate of 20 K min^{-1} and keeps isothermal for 30 min. The result shows that the bio-oil increased by 6.88 % and decreased gas yield by 7.75 %.

Keywords Empty fruit bunch · Pyrolysis · Activation energy · Coats–Redfern · Fixed-bed reactor

Introduction

Biomass waste from the palm oil processing industry in Malaysia such as empty fruit bunch (EFB) and palm shell is an exploitable source of renewable energy that is beneficial to the environment in such a way that utilization of these biomass wastes promoted reduction in the emission of carbon dioxide [1]. Due to its

A. R. Mohamed (✉) · Z. Hamzah
Complex of Engineering Studies, UniMAP, Haz Melati 1 Road, 02400 Beseri, Perlis, Malaysia
e-mail: alinamohamed@rocketmail.com

abundance, EFB is a prominent source of renewable energy and possible replacement for fossil fuel in the near future via biomass pyrolysis. This process is a thermochemical conversion through decomposition under inert environment for the production of char, bio-oil and gases [2]. Bio-oil contains aqueous and organic phases, which can be utilized as chemical feedstock or as possible fuel for stationary power [3]. The biomass pyrolysis using thermogravimetric analysis (TGA) is a fast method to generate information regarding biomass thermochemical breakdown [4]. Therefore, the biomass pyrolysis kinetics data such as the activation energy (E_a) and pre-exponential factor (Ln A) are useful in planning reactions in reactors. For the single heating rate pyrolysis, the kinetic parameters are normally determined by the Coats–Redfern method [5]. Pyrolytic reactions of various types of biomass based on the calculated E_a of kinetic parameters were reported [6–16] and also pyrolysis of biomass blended with coal [17]. The pyrolysis reaction in TGA can be improved by the addition of catalyst aimed at lowering devolatilization temperature. The integration of the catalyst during biomass pyrolysis in reactors is addressed as a significant research area in order to obtain bio-oil or pyrolysis liquid with improved fuel-like properties as well as expected to increase the yield of bio-oil [18]. The list of reported studies on catalytic pyrolysis conducted in various types of reactors with the catalysts is shown in Table 1.

It is apparent from the above reported studies (Table 1) that the selection of catalysts for catalytic pyrolysis in reactor is normally based on several factors such as catalyst acidity, basicity and porosity. The selection of catalyst using these factors required several sets of experiments with various catalysts loading ratio to biomass that consumed a lot of energy, chemicals and time. Therefore, the alternative approach suggested is aimed at utilizing the E_a values from thermogravimetric study estimated by the Coats–Redfern method for the selection of metal oxide. The catalytic reaction is expected to produce lower E_a values compared to under non-catalytic reaction that leads to the selection of a particular metal oxide catalyst for the incorporation in a fixed-bed reactor, with the aim to enhance the bio-oil yield.

Materials and methods

Biomass pretreatment

The empty fruit bunches (EFB) was obtained from palm oil mill North Star Palm Oil Mills, which is located in Kuala Ketil, Kedah, Malaysia. The biomass was rinsed with tap water to remove impurities and chopped manually. It was dried in the oven for 24 h at 343 K. The dried sample shredded using shredding machine and sieved using the Retsch sieve shaker. The sieved EFB with particle size of 250–500 μm was selected for the pyrolysis process.

Catalyst preparation

Approximately 10 g of aluminum oxide (Al_2O_3, Acros Organic, Belgium 99 % extrapure) and silica-alumina (SiO_2–Al_2O_3) catalyst support, grade 135 (Sigma-

Table 1 The list of catalytic pyrolysis of biomass performed in various types of reactors

Raw material	Catalyst	Catalyst selection basis	Improvement	Ref.
Rice stalk	Gamma-Al_2O_3 + LOSA-1	Acidic, mesoporous	Increased yield of olefin and aromatic compounds	[19]
	Cao + LOSA-1	Strong base, macropores		
	MCM-41 + LOSA-1	Mesoporous material		
Herb residue	Zeolite	Acidic cracking	Decrease oil yield, increase calorific content of oil	[20]
	Al doped SBA-15	Mesoporous material		
	Alumina	Acidic cracking	Oil yield increased, increase aliphatic content in oil	
Rapeseed cake	γ-Alumina	Acidic, enhanced secondary cracking	Pyrolysis liquid yield decreased	[21]
	HZSM-5	Acidic, shape selectivity	Pyrolysis liquid yield decreased, most effective deoxygenation	
	Na_2CO_3	Basic	Produced mostly aliphatic hydrocarbons, oil has highest calorific value	
Miscanthus x giganteus	Al_2O_3	Acidic	Increased bio-oil yield, higher aliphatic and aromatic compound content	[22]
Euphorbia rigida	DHC-32	Commercial catalyst	Increased bio-oil yield	[23]
Sesame stalk	HCK-1.3Q			
Cotton seed	MgO	Basic	Increased bio-oil yield	[24]
Hazelnut shell	Red mud	Mixture of metal oxides	No distinct effect on gas generation	[25]
	HZSM-5	Microporous, shape-selectivity catalyst	Bio-oil contained furans, acids and aldehydes	
	K_2CO_3	Basic	Bio-oil has etheric structure	
	SnO_2 nanoparticles	Increased surface area	Highest gas yield	
Pistacia khinjuk seed	BP 3189	Commercial catalyst	increased bio-oil yield	[26]
	Criterion-424 (Ni–Mo)			

Table 1 continued

Raw material	Catalyst	Catalyst selection basis	Improvement	Ref.
Hazelnut bagasse Olive waste	Activated alumina Sodium feldspar	Acidic	Higher calorific value of bio-oil with low oxygen content but high hydrogen to carbon (H/C) ratio.	[27]
Lignocell, Miscanthus	Al-MCM-41	Mesoporous molecular sieve, large surface area	Aliphatic hydrocarbon and polycyclic aromatic hydrocarbon (PAHs) contents increased	[28]
	Fe-MCM Cu-MCM Zn-MCM		Aliphatic hydrocarbon content decreased	
EFB	Boric oxide	Structural flexibility	Increased char yield, reduced gas yield, had deoxygenation effect	[29]
Empty palm fruit bunch (EPFB)	HZSM-5 HY	Acidic cracking catalyst	Higher phenolic content in bio-oil	[30]
	Al-MCM-41	Mesoporous, larger surface area	Eliminated the acid content in bio-oil	

Aldrich, Germany) were calcined separately in a furnace at 923 K for 5 h at a ramp rate of 3 K min^{-1} [31] under static atmosphere and the catalysts were placed in a desiccators prior to application.

Alumina doped with Cu, Ni and Co was prepared using the wet impregnation technique [31]. 10 ml of deionized water was measured and poured into a beaker. A pre-weighed respective amount of nitrate salt of Cu, Ni and Co ($Cu(NO_3)\cdot 3H_2O$ (R&M Chemicals, UK), $Ni(NO_3)_2\cdot 6H_2O$ (Merck, Germany) and $Co(NO_3)_2\cdot 6H_2O$ (Merck, Germany)) with atomic ratio to alumina of 5 % dissolved with deionized water. The solution containing the respective ion was added dropwise into a beaker containing 10.00 g of precalcined alumina until about 60 % of solution was transferred. It was dried at room temperature for about 5 h. The remaining solution was subsequently added. It was left to dry overnight. It was again dried at 393 K for 2 h. Then, the catalyst precursor was calcined at 873 K for 5 h at a ramp rate of 3 K min^{-1}.

Catalytic and non-catalytic biomass pyrolysis using a thermogravimetric analyzer (TGA)

The non-catalytic and catalytic pyrolysis was conducted using Mettler Toledo thermal analyzer TGA/DSC 1 equipped with Star^e software. In non-catalytic pyrolysis condition, approximately 10.00 mg of sample was placed in a 70 µl alumina crucible. In catalytic condition, approximately 1.00 mg of alumina catalyst was weighed and placed inside the crucible containing 10.00 mg EFB to produce 9.09 wt% catalyst addition to biomass. The nitrogen gas was used as the carrier gas at a flow rate of 100 ml min^{-1} under dynamic conditions from 301 K towards final pyrolysis temperature of 1,273 K at a heating rate of 10 K min^{-1}. Each heating rate produced data Excel spreadsheet and the data was calculated using Excel software with the Coats–Redfern method. The presented experimental data were the mean values calculated from three replicated experiments under the same operating conditions. The data showed good reproducibility and repeatability.

Kinetic analysis by Coats–Redfern method

The pyrolysis process of EFB could be represented by this reaction scheme:

$$\text{EFB solid residue} + \text{volatiles} \tag{1}$$

The rate of pyrolysis process in kinetic study was deduced as:

$$\frac{d\alpha}{dt} = kf(\alpha) \tag{2}$$

In this equation, α is the progress of reaction or the conversion and it occurred from 0.05 to 0.95. The value of α could be defined as:

$$\begin{aligned} \alpha &= \frac{w_o - w_t}{w_o - w_f} \\ f(\alpha) &= (1-\alpha)^n \end{aligned} \tag{3}$$

The rate constant depended on the activation energy (E_a).

$$k = A \exp\left(-\frac{E_a}{RT}\right) \tag{4}$$

When Eqs. 2 and 4 are combined, a new equation is obtained as follows:

$$\frac{d\alpha}{dt} = A \exp\left(-\frac{E_a}{RT}\right) f(\alpha) \tag{5}$$

A new parameter called heating rate (B) was introduced when the EFB pyrolysis reaction was performed under dynamic non-isothermal condition.

$$\beta = \frac{dT}{dt} \text{ or } dt = \frac{dT}{\beta} \tag{6}$$

Insertion of Eq. 6 into Eq. 5 produced Eq. 7:

$$\begin{aligned} \frac{d\alpha}{(dT/\beta)} &= A \exp\left(-\frac{E_a}{RT}\right) f(\alpha) \\ \frac{d\alpha}{(dT)} &= \frac{A}{\beta} \exp\left(-\frac{E_a}{RT}\right) f(\alpha) \end{aligned} \tag{7}$$

Equations 5 and 7 were the basic equations that could be used to generate kinetic parameters that utilized the thermogravimetric data obtained either at linear heating rates, β or at selected heating rate.

$$\ln\left[-\frac{\ln(1-\alpha)}{T^2}\right] = \ln\left[\frac{AR}{\beta E_a}\left[1 - \frac{2RT}{E_a}\right]\right] - \frac{E}{RT} \tag{8}$$

The Coats–Redfern method was being used to calculate the activation energy (E_a) and pre-exponential factor (Ln A) from the catalytic and non-catalytic pyrolysis of biomass [32–34]. The equation is applicable when the reaction order (n) equals to 1.

Catalytic pyrolysis in a fixed-bed reactor

The catalytic pyrolysis of EFB with alumina was carried out in a vertical fixed-bed reactor placed in an electrical furnace. In a typical pyrolysis run, approximately 10.00 g of EFB was mixed with alumina at 9.09 wt% at in-bed mode. The catalyst loading was varied at 9.09, 16.67 and 23.08 wt%. The reactor was purged with nitrogen at 300 ml min^{-1} for 30 min to ensure inert environment during the pyrolysis. The final pyrolysis temperature was set at 773 K with a heating rate of 20 K min^{-1} and maintained at that temperature for 30 min. The pyrolysis products were swept by nitrogen and passed through a condenser and the receiver flask was immersed in a mixture of ice and water. The flask was weighed before and after the reaction. Thus, the bio-oil yield was determined by difference. The solid residue was removed from the reactor tube and its weight was recorded. Each experiment

was conducted in duplicate in order to provide standard deviation of ±3.0 wt%. The mean values were considered for analysis. The relevant calculations are as shown in Eqs. 9, 10, 11 and 12.

$$\text{Conversion } (\%) = \frac{mass\ of\ EFB\ (\text{g}) - mass\ of\ charresidue\ (\text{g})}{mass\ of\ EFB(\text{g})} \times 100\ \% \quad (9)$$

$$\text{Bio-oil yield } (\text{wt}\%) = \frac{mass\ of\ bio{-}oil\ (\text{g})}{mass\ of\ EFB\ (\text{g})} \times 100\ \% \quad (10)$$

$$\text{Char residue yield } (\text{wt}\%) = \frac{mass\ of\ char\ residue\ (\text{g})}{mass\ of\ EFB\ (\text{g})} \times 100\ \% \quad (11)$$

$$\text{Gas yield } (\text{wt}\%) = 100(\text{wt}\%) - \text{bio-oil yield } (\text{wt}\%) - \text{char residue } (\text{wt}\%) \quad (12)$$

Results and discussion

TG and DTG analysis

The TG curves for catalytic and non-catalytic EFB pyrolysis at a heating rate of 10 K min^{-1} are depicted in Fig. 1a and b. The curve is divided into three different stages. The first stage corresponded to the slight weight loss that occurred in the temperature range from room temperature to 473 K due to the removal of moisture of biomass [35]. The second stage referred to the successive decomposition of lignocellulosic components of EFB at temperature region of 473–673 K, where devolatilization of lignin, cellulose and hemicellulose components contained in biomass took place. Therefore, biomass cracking reactions such as depolymerization, decarbonylation and decarboxylation took place at this temperature region. The slow weight loss or flat tailing section at temperature region of 673–1,073 K was attributed to the decomposition of lignin, which was known to degrade slowly over large range of temperature [36]. The final char yield in EFB pyrolysis was in the range of 21.34–22.10 %. However, there was an increase to 25.92–38.85 % in the presence of metal oxide catalysts was recorded. This indicated that the presence of catalysts increased the char yield at the end of pyrolysis process. Similar observations were reported by Shurong Wang et al. [37]. Fe^{2+} and K^{+} increased the final char residue of cellulose pyrolysis as well as shifted the cellulose devolatilization peak in DTG curve towards low-temperature thus reduced the E_a of the pyrolysis process [37]. The presence of $MgCl_2$ impregnated cellulose also promoted the char production in catalytic $MgCl_2$-cellulose pyrolysis [38].

The DTG curves for both EFB pyrolysis and catalytic EFB pyrolysis are shown in Fig. 2. The initial small peak was recorded in the range of approximately 323–423 K due to the expulsion of physisorbed water molecules [39]. The main EFB lignicellulosic decomposition cracking reactions occurred in the temperature range from 473 to 673 K. The main DTG peak at approximately 610 K in EFB pyrolysis was due to the contribution from the cellulose decomposition. The largest

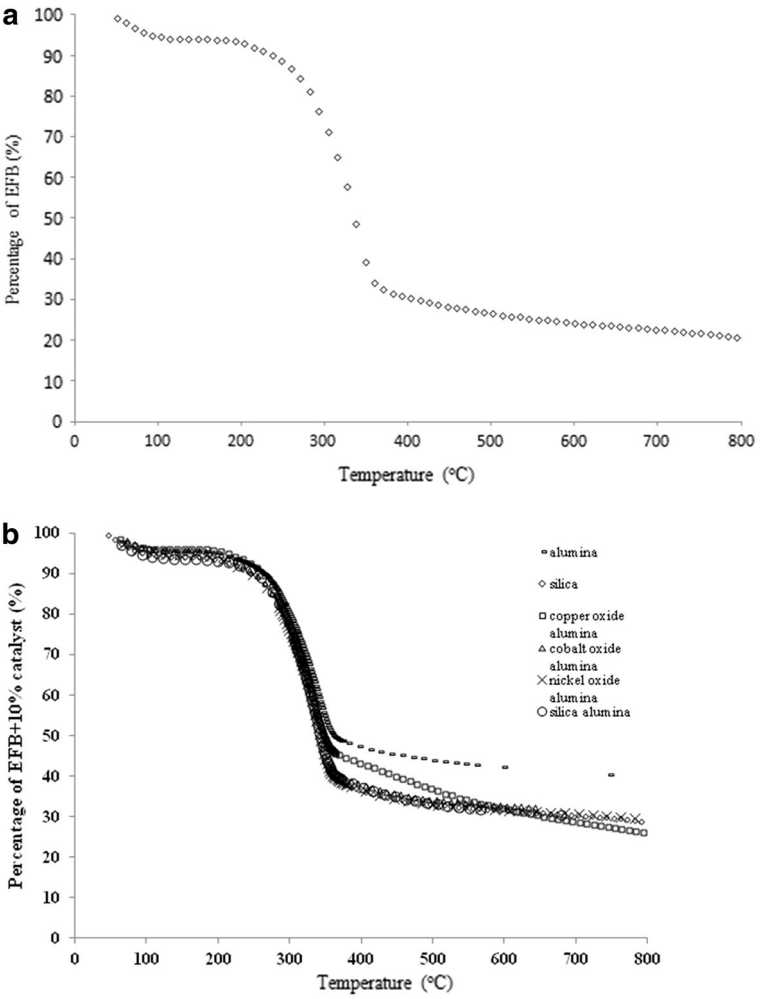

Fig. 1 **a** TG curves for EFB pyrolysis conducted under nitrogen atmosphere at a flow rate of 100 ml min^{-1} from 28 to 1,000 °C (301–1,273 K) at a heating rate of 10 K min^{-1}. **b** TG curves for catalytic EFB pyrolysis conducted under nitrogen atmosphere at a flow rate of 100 ml min^{-1} from 28 to 1,000 °C (301–1,273 K) at a heating rate of 10 K min^{-1}

peak which was a signal of cellulose decomposition from waste mandarin residue pyrolysis appeared in the temperature range of 593–653 K [12], while cellulose decomposition was reported to occur in the temperature range of 550–670 K [39]. The main DTG peak was accompanied by a shoulder peaked at approximately 560–573 K in both catalytic and non-catalytic pyrolysis of EFB. This shoulder peak corresponded to the devolatilization of hemicellulosic component of EFB.

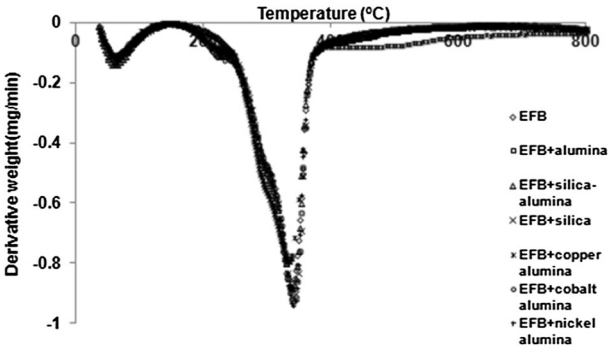

Fig. 2 DTG curves for EFB pyrolysis and catalytic EFB pyrolysis conducted under nitrogen atmosphere at a flow rate of 100 ml min^{-1} from 28 to 1,000 °C (301–1,273 K) at a heating rate of 10 K min^{-1}

Kinetic analysis based on Coats–Redfern method

Based on the DTG analysis on the EFB sample under catalytic and non-catalytic condition, the peak temperature for cellulose pyrolysis was slightly lower than 613 K. Therefore, in the current study, the temperature region of 473–573 K is considered as section I, which accounted for hemicellulose decomposition. The temperature range of 573–613 K is regarded as section II that corresponded to the cellulosic degradation. This temperature regime selection is similar to Yang et al. [40]. Yang et al. [40] conducted the pyrolysis of cellulose, hemicelluloses and lignin as well as palm oil wastes such as EFB and palm shell. The xylan (mainly hemicellulose) decomposition occurred in the temperature region of 493–573 K. Meanwhile cellulose degradation occurred in the temperature range of 573–613 K.

Sections I and II from the non-catalytic and catalytic pyrolysis of EFB conformed to first order reactions. The plot of $\ln[-\ln(1-\alpha)/T^2]$ against 1/T produced linear curves with the slope equals to E_a/R. Concomitantly, the E_a and Ln A can be determined. The linear curves producing linear equations with R^2 values for sections I and II are as recorded in Tables 2 and 3. The values of estimated standard errors for kinetic parameters such as E_a and Ln A are shown in Tables 2 and 3. The values of calculated R^2 are above 0.96 which indicated the acceptable correlation between the dependable and non-dependable parameters.

The differences between the values of mean E_a from catalytic with non-catalytic EFB pyrolysis are shown in Figs. 3 and 4 for sections I and II, respectively.

The mean E_a for EFB pyrolysis is 94.41 kJ mol^{-1} with the range of 90.38–96.68 kJ mol^{-1} in the first step reaction or section I. The incorporation of Al_2O_3 and SiO_2 into EFB pyrolytic reaction had positively reduced the values of mean E_a by 6.05 and 2.10 kJ mol^{-1}, respectively. Thus, the heights of Al_2O_3 and SiO_2 catalyzed reaction as shown in Fig. 3 are slightly lower than the non-catalyzed EFB pyrolysis reaction. The respective ranges of E_a were 86.29–89.74 and 87.51–96.94 kJ mol^{-1} for Al_2O_3 and SiO_2 catalyzed reactions. However, the reverse is observed when SiO_2–Al_2O_3 catalyst is used that the values of E_a increases by 4.59 kJ mol^{-1} in the range of 109.67–115.22 kJ mol^{-1}. The utilization of doped

Table 2 The kinetic parameters (activation energy and Ln A) from EFB pyrolysis reaction for section I (hemicellulose decomposition) for range of α value from 0.05 to 0.90

Reaction	Equation	R^2	Ea (kJ mol^{-1})	Ln A	Mean Ea	Mean LnA	Estimated standard error for Ea	Estimated standard error for Ln A
EFB pyrolysis	$y = -11629x + 8.2535$	0.97	96.68	16.61	94.41	16.13	2.02	0.48
	$y = -11566x + 8.2361$	0.98	96.16	16.59				
	$y = -10871x + 6.876$	0.98	90.38	15.17				
EFB + Al_2O_3	$y = -10712x + 6.6096$	0.98	89.06	14.89	88.36	15.12	1.06	0.60
	$y = -10379x + 5.9776$	0.98	86.29	14.22				
	$y = -10794x + 6.8779$	0.98	89.74	16.26				
EFB + SiO_2–Al_2O_3	$y = -13708x + 12.012$	0.99	113.97	20.54	112.95	20.83	1.68	0.41
	$y = -13859x + 12.267$	0.99	115.22	21.64				
	$y = -13191x + 10.939$	0.97	109.67	20.31				
EFB + SiO_2	$y = -10526x + 6.2407$	0.97	87.51	14.50	92.31	16.35	2.72	0.96
	$y = -11124x + 7.4826$	0.99	92.48	16.86				
	$y = -11660x + 8.3186$	0.96	96.94	17.70				
EFB + CuO/Al_2O_3	$y = -12029x + 9.0444$	0.98	100.01	17.31	94.31	16.81	2.89	0.27
	$y = -11093x + 7.353$	0.97	92.23	16.73				
	$y = -10908x + 7.0205$	0.97	90.69	16.39				
EFB + CoO/Al_2O_3	$y = -11556x + 8.1283$	0.97	96.08	16.39	96.33	17.92	0.72	0.45
	$y = -11453x + 7.9889$	0.97	95.22	17.36				
	$y = -11749x + 8.568$	0.98	97.68	17.92				
EFB + NiO/Al_2O_3	$y = -11223x + 7.6619$	0.98	93.31	15.92	92.73	16.47	3.48	0.78
	$y = -11842x + 8.6406$	0.97	98.45	18.01				
	$y = -10397x + 6.1026$	0.99	86.44	15.48				

Table 3 Calculated kinetic parameters (activation energy and Ln A) from EFB pyrolysis reaction for section II (cellulose decomposition) for range of α value from 0.05 to 0. 91 (temp range 573–613 K)

Reaction	Equation	R^2	Ea (kJ mol^{-1})	Ln A	Mean Ea	Mean LnA	Estimated standard error for Ea	Estimated standard error for Ln A
EFB	y = −32167x + 40.77	0.98	267.44	50.16	266.14	49.87	0.66	0.15
	y = −31953x + 40.40	0.98	265.66	49.77				
	y = −31913x + 40.32	0.98	265.32	49.69				
EFB + Al_2O_3	y = −31496x + 39.70	0.98	261.86	49.05	264.37	49.52	1.31	0.25
	y = −31882x + 40.25	0.98	265.07	49.62				
	y = −32022x + 40.51	0.98	266.23	49.88				
EFB + SiO_2–Al_2O_3	y = −31959x + 40.43	0.98	265.71	48.96	262.03	48.80	2.10	0.21
	y = −31501x + 39.68	0.98	261.90	49.05				
	y = −31089x + 39.02	0.97	258.47	48.39				
EFB + SiO_2	y = −31338x + 39.32	0.98	260.54	47.58	263.91	49.03	2.31	0.80
	y = −32273x + 40.94	0.98	268.32	50.32				
	y = −31618x + 39.83	0.98	262.87	49.20				
EFB + CuO/Al_2O_3	y = −31820x + 40.29	0.97	264.55	48.55	264.64	49.23	0.61	0.36
	y = −31709x + 39.99	0.98	263.63	49.36				
	y = −31962x + 40.42	0.98	265.73	49.79				
EFB + CoO/Al_2O_3	y = −31748x + 40.10	0.98	263.95	48.36	263.93	49.08	0.29	0.37
	y = −31683x + 39.95	0.98	263.41	49.33				
	y = −31806x + 40.19	0.98	264.43	49.56				
EFB + NiO/Al_2O_3	y = −31702x + 39.94	0.98	263.57	48.20	264.29	49.14	2.21	0.64
	y = −31378x + 39.49	0.98	260.88	48.86				
	y = −32287x + 40.99	0.98	268.44	50.36				

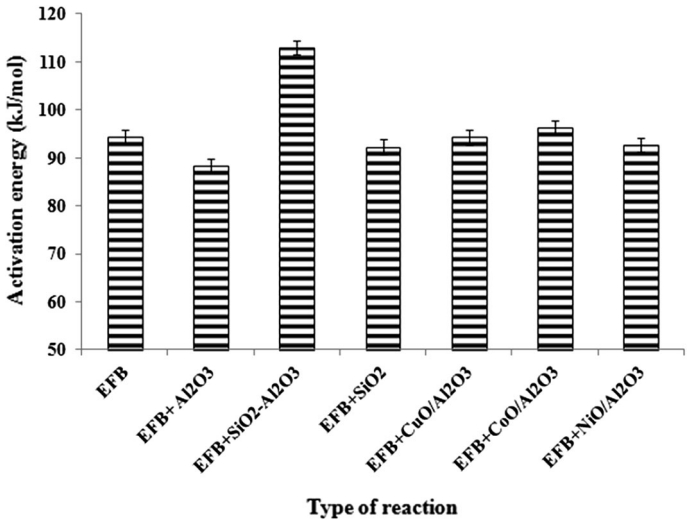

Fig. 3 The difference between calculated mean activation energy values for section I EFB catalytic and non-catalytic pyrolysis conducted under nitrogen atmosphere at a flow rate of 100 ml min^{-1} from 28 to 1,000 °C (301–1,273 K) at a heating rate of 10 K min^{-1}

Al_2O_3 such as CuO/Al_2O_3, NiO/Al_2O_3 and CoO/Al_2O_3 do not have significant effect on E_a reduction with the values of E_a ranges of 90.69–100.01, 86.44–98.45 and 95.22–97.68 kJ mol^{-1}. This is because the differences of E_a between EFB non-catalyzed reaction and CuO/Al_2O_3 and NiO/Al_2O_3 catalyzed reaction are 0.10 and 1.68 kJ mol^{-1}, respectively. This is clearly seen as a similar in heights of CuO/Al_2O_3, NiO/Al_2O_3 and CoO/Al_2O_3 catalyzed reactions with EFB non-catalyzed reactions (Fig. 3).

E_a is normally defined as the minimum energy barrier that has to be overcome in order for reaction to proceed [17]. Thus lower E_a is more preferable than high ones because the reaction become more reactive with higher sensitivity [9]. Therefore, the order of reaction reactivity between doped and undoped catalysts towards EFB pyrolysis including non-catalytic EFB pyrolysis with regard to hemicelluloses degradation as follows: EFB + Al_2O_3 > EFB + SiO_2 > EFB + NiO/Al_2O_3 > EFB + CuO/Al_2O_3 > EFB > EFB + CoO/Al_2O_3 > EFB + SiO_2–Al_2O_3.

The contribution of the catalysts used had promoted the reaction of hemicellulose pyrolysis via different routes that did not follow the non-catalytic EFB pyrolysis. The hemicellulose decomposition reaction was actually a multi-step reaction [32].

Section II was the second-step reaction, which corresponded to the cellulose degradation in EFB pyrolysis with mean E_a of 266.14 kJ mol^{-1} and in the range of 265.32–267.44 kJ mol^{-1}. Fig. 4 illustrates that all the catalyzed EFB pyrolysis reactions give lower E_a as compared to non-catalyzed EFB reaction. The addition of undoped Al_2O_3, SiO_2–Al_2O_3 and SiO_2 had reduced E_a by 1.77, 4.11 and

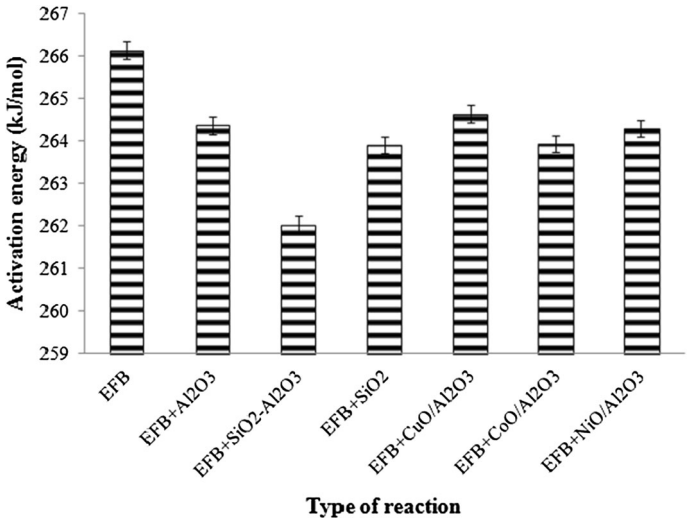

Fig. 4 The difference between calculated mean activation energy values for section I EFB catalytic and non-catalytic pyrolysis conducted under nitrogen atmosphere at a flow rate of 100 ml min^{-1} from 28 to 1,000 °C (301–1,273 K) at a heating rate of 10 K min^{-1}

2.22 kJ mol^{-1} with the ranges of E_a are 261.86–266.23, 258.47–265.41 and 260.54–268.32 kJ mol^{-1}. Among these, SiO_2–Al_2O_3 is more active than the other two catalysts.

While for doped catalysts such as CuO/Al_2O_3, CoO/Al_2O_3 and NiO/Al_2O_3, a slight reduction in E_a of 1.50, 2.21 and 1.85 kJ mol^{-1} was determined with E_a ranges of 263.63–265.73, 263.41–264.43 and 260.88–268.44 kJ mol^{-1}. The order of reaction reactivity towards cellulosic degradation in EFB pyrolysis considering both catalytic and non-catalytic reactions is as follows: EFB + SiO_2–Al_2O_3 > EFB + SiO_2 > EFB + CoO/Al_2O_3 > EFB + NiO/Al_2O_3 > EFB + Al_2O_3 > EFB + CuO/Al_2O_3 > EFB.

In general, the mean E_a values for section I are much lower as compared to the mean E_a in section II for both EFB pyrolysis and catalytic EFB pyrolysis. This might be due to the fact that the content of volatiles released was lower [5] in section I as compared to section II. In addition, cellulose itself possessed semi-crystalline structure in comparison to hemicelluloses that were non-crystalline. Therefore, higher amount of energy was needed to breakdown the crystal structure which in turn resulted in higher E_a [41].

Alumina and silica-alumina were considered as acidic catalyst material which promoted the biomass pyrolysis via decarbonylation reaction [42]. It was expected that by doping alumina with copper oxide, cobalt oxide and nickel oxide, the E_a for EFB pyrolysis could be further reduced. According to Chattopadhyay et al. [4], the combination between spinel structure Cu/Al_2O_4 and small amounts of Cu_2O observed by X-ray diffraction seemed active in reducing the devolatilization temperature of paper pyrolysis. However, in the current study, the CuO/Al_2O_3 and NiO/Al_2O_3 catalysts have no significant effect in reducing the mean E_a for

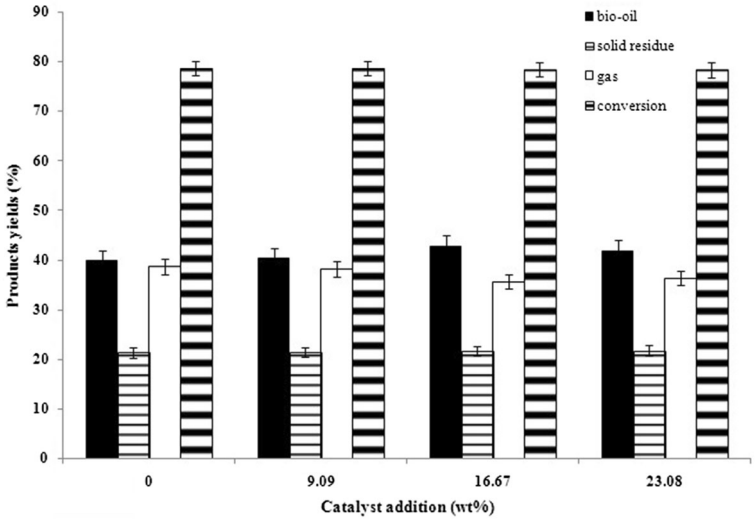

Fig. 5 The effect of alumina catalyst loading on the EFB pyrolysis products yields conducted in a fixed-bed reactor at 773 K with a heating rate of 20 K min^{-1} and maintained at that temperature for 30 min

hemicellulose decomposition in EFB pyrolysis. This could be due to various factors such as the catalyst preparation method, catalyst to biomass ratio, the percentage of copper loading within alumina based and the presence of phase that formed during catalyst preparation stage. The investigation by X ray diffraction on the prepared catalysts could provide some information on the catalyst active sites that exist on the surface of the catalyst. From the study, it can be concluded that Al_2O_3 and SiO_2 are prominent undoped metal oxide catalysts in EFB hemicellulose decomposition because the E_a values are lower compared to non-catalyzed EFB pyrolysis. All catalyst showed good catalytic activity in cellulose decomposition of EFB because the mean Ea values are reduced in the presence of these catalysts.

Catalytic pyrolysis of EFB with alumina in a fixed-bed reactor

Figure 5 shows the pyrolysis product yields against the catalyst loading from the catalytic EFB pyrolysis with Al_2O_3 in the fixed-bed reactor at a programmed rate of 20 K min^{-1} towards a final pyrolysis temperature of 773 K under nitrogen environment with a flow rate of 300 ml min^{-1}.

There is no distinctive change in the reaction conversion since it is in the range of 78.3–78.65 % when the Al_2O_3 catalyst is increased. This finding seems to be in contradiction with Yorgun and Simsek [22] which reported that the reaction conversion of *Miscanthus x giganteus* in catalytic Al_2O_3 reaction was on increasing trend when the Al_2O_3 amount was increased. This is because the increasing alumina provided increasing number of active sites which were responsible for catalytic cracking reactions such as depolymerization and deoxygenation [22]. In the current study, the Al_2O_3 catalyst effect can be observed through the mean bio-oil and gas yield obtained since the reaction conversion shows no significant change.

It is determined that the bio-oil yield rises but gas yield reduced in conjunction with increasing catalyst addition and reaches its maximum and minimum of 42.70 and 35.70 wt% with using 16.67 wt% Al_2O_3 catalyst. However, the bio-oil yield reduces when more catalyst is added. The obtainment of 42.70 wt% bio-oil yield was comparable to other reported studies such as by Wang et al. [20] and Yorgun and Simsek [22]. This study indicated that the incorporation of Al_2O_3 into the biomass catalytic pyrolysis had positively increased bio-oil yield since the bio-oil was increased by 6.88 % and reduced gas yield by 7.75 % when 16.67 wt% was added.

There is no change in terms of char residue yield when Al_2O_3 catalyst is increased. This seems to be in good agreement with reported study by Demiral and Sensoz [27]. On the contrary, Wang et al. [20] reported that the SBA-15 and alumina catalyst had decreased the solid products from the pyrolysis of herb residue performed in a horizontal quartz reactor.

These observations of increasing bio-oil yield, reducing gas yield and no change in char residue under increasing Al_2O_3 catalytic reaction are might be due to the successful primary reactions and inhibition of the secondary reactions. A good indication of the occurrence of secondary reaction is the reduction in char residue, as well as increasing gas and reducing bio-oil yields [43], which resulted from the reaction between the hot-biochar fraction with the newly formed hot vapors that underwent further decomposition reaction due to high temperature effect [44]. These are not observed in the current study which indicated that the incorporation of alumina catalyst at 773 K is advantageous towards increasing the bio-oil yield, reduced gas yield and inhibition of secondary pyrolytic reaction for promotion of the primary reactions.

Conclusion

The values of E_a from non-catalytic and catalytic EFB thermogravimetric pyrolysis with a series of metal oxide catalysts were estimated with reference to the Coats–Redfern method for the selection of a metal oxide catalyst. It was identified that Al_2O_3 catalyzed EFB pyrolysis had reduced the hemicellulose decomposition by 6.05 kJ mol^{-1}.

The incorporation of Al_2O_3 in catalytic EFB pyrolysis a fixed bed reactor at 773 K increased the bio-oil yield by 6.88 % and decreased gas yield by 7.75 %.

Acknowledgments The authors would like to acknowledge the Malaysian Ministry of Higher Education for the financial assistance in terms of Fundamental Research Grant Scheme (FRGS) and Mr Teoh from Norstar Palm Oil Mill in Kuala Ketil, Kedah, Malaysia for supplying EFB for this research.

References

1. Sulaiman F, Abdullah N, Gerhauser H, Shariff A (2011) An outlook of Malaysian energy, oil palm industry and its utilization of wastes as useful resources. Biomass Bioenergy 35:3775–3786
2. Demirbas MF, Balat M (2007) Biomass pyrolysis for liquid fuels and chemicals: a review. J Sci Ind Res India 66:797–804

3. Huber GW, Iborra S, Corma A (2006) Synthesis of transportation fuels from biomass: chemistry, catalysts, and engineering. Chem Rev 106:4044–4098
4. Chattopadhyay J, Kim C, Kim R, Pak D (2009) Thermogravimetric study on pyrolysis of biomass with Cu/Al_2O_3 catalysts. J Ind Eng Chem 15:72–76
5. Vlaev LT, Markovska IG, Lyubchev LA (2003) Non-isothermal kinetics of pyrolysis of rice husk. Thermochima Acta 406:1–7
6. Chutia RS, Kataki R, Bhaskar T (2013) Thermogravimetric and decomposition kinetic studies of *Mesua ferrea deoiled cake*. Bioresour Technol 139:66–72
7. Yao F, Wu Q, Lei Y, Guo W, Yanjun Xu (2008) Thermal decomposition kinetics of natural fibers: activation energy with dynamic thermogravimetric analysis. Polym Degrad Stab 93:90–98
8. Ounas A, Aboulkas A, Elharfi K, Bacaoui A, Yaacoubi A (2011) Pyrolysis of olive residue and sugarcane bagasse: non-isothermal thermogravimetric kinetic analysis. Bioresour Technol 102:11234–11238
9. Wongsiriamnuay T, Tippayawong N (2010) Non-isothermal pyrolysis characteristics of giant sensitive plants using thermogravimetric analysis. Bioresour Technol 101:5638–5644
10. Haykiri-Acma H (2006) The role of particle size in the non-isothermal pyrolysis of hazelnut shell. J Anal Appl Pyrolysis 75:211–216
11. Yang H, Yan R, Liang DT, Chen H, Zheng C (2006) Pyrolysis of palm oil wastes for biofuel production. Asian J Energy Environ 7(02):315–323
12. Kim JW, Lee S-H, Kim S-S, Park SH, Jeon J-K, Park Y-K (2011) The pyrolysis of waste mandarin residue using thermogravimetric analysis and a batch reactor. Korean J Chem Eng 28(9):1867–1872
13. Gao W, Chen K, Xiang Z, Yang F, Zeng J, Li J, Yang R, Rao G, Tao H (2013) Kinetic study on pyrolysis of tobacco residues from the cigarette industry. Ind Crop Prod 44:152–157
14. Luo G, Strong PJ, Wang H, Ni W, Shi W (2011) Kinetics of the pyrolytic and hydrothermal decomposition of water hyacinth. Bioresour Technol 102:6990–6994
15. Gottipati R, Mishra S (2011) A kinetic study on pyrolysis and combustion characteristics of oil cakes: effect of cellulose and lignin content. J Fuel Chem Technol 39(4):265–270
16. Poletto M, Dettenborn J, Pistor V, Zeni M, Zattera AJ (2010) Materials produced from plant biomass. Part 1: evaluation of thermal stability and pyrolysis of wood. Mater Res 13(3):375–379
17. Idris SS, Rahman NA, Ismail K, Alias AB, Rashid ZA, Aris MJ (2010) Investigation on thermochemical behavior of low rank Malaysian coal, oil palm biomass and their blends during pyrolysis via thermogravimetric analysis (TGA). Bioresour Technol 101:4584–4592
18. Hu C, Yang Y, Luo Z, Pan P, Tong D, Li G (2011) Recent advances in the catalytic pyrolysis of biomass. Front Chem Sci Eng 5(2):188–193
19. Zhang H, Xiao, Jin B, Xiao G, Chen R (2013) Biomass catalytic pyrolysis to produce olefins and aromatics with a physically mixed catalyst. Bioresour Technol 140:256–262
20. Wang P, Zhan S, Yu H, Xue X, Hong N (2010) The effects of temperature and catalysts on the pyrolysis of industrial wastes (herb residue). Bioresour Technol 101:3236–3241
21. Smets K, Roukaerts A, Czech J, Reggers G, Schreurs S, Carleer R, Yperman J (2013) Slow catalytic pyrolysis of rapeseed cake: product yield and characterization of the pyrolysis liquids. Biomass Bioenergy 57:180–190
22. Yorgun S, Simsek YE (2008) Catalytic pyrolysis of *Miscanthus giganteus* over activated alumina. Bioresour Technol 99:8095–8100
23. Ates F, Putun AE, Putun E (2006) Pyrolysis of two different biomass samples in a fixed-bed reactor combined with two different catalysts. Fuel 85:1851–1859
24. Putun E (2010) Catalytic pyrolysis of biomass: effect of pyrolysis temperature, sweeping gas flowrate and MgO catalyst. Energy 35:2761–2766
25. Gokdai Z, Sinag A, Yumak T (2010) Comparison of the catalytic efficiency of synthesized nano tin oxide particles and various catalysts for the pyrolysis of hazelnut shell. Biomass Bioenergy 34:402–410
26. Onay O (2007) Fast and catalytic pyrolysis of *pistacia khinjuk* seed in a well-swept fixed bed reactor. Fuel 86:1452–1460
27. Demiral I, Sensoz S (2008) The effects of different catalysts on the pyrolysis of industrial wastes (olive and hazelnut bagasse). Bioresour Technol 99:8002–8007
28. Antonakou E, Lappas A, Nilsen MH, Bouzga A, Stocker M (2006) Evaluation of various types of Al-MCM-41 materials as catalysts in biomass pyrolysis for the production of bio-fuels and chemicals. Fuel 85:2202–2212

29. Lim XY, Andresen JM (2011) Pyro-catalytic deoxygenated bio-oil from palm oil empty fruit bunch and fronds with boric oxide in a fixed-bed reactor. Fuel Proc Technol 92:1796–1804
30. Misson M, Haron R, Kamaroddin MFA, Amin NAS (2009) Pretreatment of empty palm fruit bunch for production of chemicals via catalytic pyrolysis. Bioresour Technol 100(11):2867–2873
31. Zabeti M, Nguyen TS, Lefferts L, Heeres HJ, Seshan K (2012) In situ catalytic pyrolysis of lignocellulose using alkali-modified amorphous silica alumina. Bioresour Technol 118:374–381
32. Lu C, Song W, Lin W (2009) Kinetics of biomass catalytic pyrolysis. Biotechnol Adv 27:583–587
33. Shih Y-F (2007) A study of the fiber obtained from the water bamboo husks. Bioresour Technol 98:819–828
34. Tonbul Y (2008) Pyrolysis of pistachio shell as a biomass. J Therm Anal Calorim 91(2):641–647
35. Ertaş M, Alma MH (2010) Pyrolysis of laurel (*Laurus nobilis* L.) extraction residues in a fixed-bed reactor: characterization of bio-oil and bio-char. J Anal Appl Pyrolysis 88(1):22–29
36. Hu S, Jess A, Xu M (2007) Kinetic study of Chinese biomass slow pyrolysis: comparison of different kinetic models. Fuel 86:2778–2788
37. Wang S, Liu Q, Liao Y, Luo Z, Cen K (2007) A study on the mechanism research on cellulose pyrolysis under catalysis of metallic salts. Korean J Chem Eng 24(2):336–340
38. Khelfa A, Finqueneisel G, Auber M, Weber JV (2008) Influence of some minerals on the cellulose thermal degradation mechanisms: thermogravimetry and pyrolysis-mass spectrometry studies. J Therm Anal Calorim 92(3):795–799
39. Shurong W, Qian L, Zhongyang L, Lihua W, Kefa C (2007) Mechanism study on cellulose pyrolysis using thermogravimetric analysis coupled with infrared spectroscopy Front. Energy Power Eng China 1(4):413–419
40. Yang H, Yan R, Chin T, Liang DT, Chen H, Zheng C (2004) Thermogravimetric analysis–fourier transform infrared analysis of palm oil waste pyrolysis. Energy Fuels 18(6):1814–1821
41. Jiang G, Nowakowski DJ, Bridgwater AV (2010) A systematic study of the kinetics of lignin pyrolysis. Thermochim Acta 498:61–66
42. Stefanidis SD, Kalogiannis KG, Iliopoulou EF, Lappas AA, Pilavachi PA (2011) In-situ upgrading of biomass pyrolysis vapors: catalyst screening on a fixed bed reactor. Bioresour Technol 102:8261–8267
43. Duman G, Okutucu C, Ucar S, Stahl R, Yanik J (2011) The slow and fast pyrolysis of cherry seed. Bioresour Technol 102:1869–1878
44. Neves D, Thunman H, Matos A, Tarelho L, Gómez-Barea A (2011) Characterization and prediction of biomass pyrolysis products. Prog Energy Combust Sci 37:611–630